AIAA JOURNAL
Vol. 40, No. 5, May 2002

Instability of Accelerated Boundary Layers Induced by Surface Suction

P. J. D. Roberts* and J. M. Floryan†
University of Western Ontario, London, Ontario N6A 5B9, Canada

Accelerated boundary layers are considered to be stable for practical purposes. It is shown that small suction nonuniformities can induce an instability that results in the generation of streamwise vortices. Addition of a uniform suction is not effective in controlling this instability. It is shown that nonuniformities of surface blowing might induce a similar instability and that the characteristics of this instability are also little affected by the magnitude of the blowing. The same nonuniformities appear to have a small effect on the traveling (Tollmien–Schlichting) wave instability in the range of parameters studied. It is shown that oblique waves become dominant if the amplitudes of the nonuniformities become large enough.

Nomenclature

A_{nk}	=	coefficient matrix [Eq. (10)]
c_n	=	arbitrary constants [Eq. (7)]
$D = \mathrm{d}/\mathrm{d}y$	=	derivative operator
F	=	similarity function in the Falkner–Skan equation
$\bar{G}_m = [g_u^{(m)}, g_w^{(m)}, g_v^{(m)}]$	=	disturbance amplitude field
M	=	number of Fourier modes
N	=	number of Chebyshev polynomials
Re	=	Reynolds number
Re_s	=	suction Reynolds number
S	=	amplitude of suction nonuniformity
$t_m, k_m, T^{(m)}, S^{(m)}, N_u^{(m)}, N_w^{(m)}, N_v^{(m)}, K_u^{(m)}, K_w^{(m)}, K_v^{(m)}, L_u^{(m)}, L_w^{(m)}, L_v^{(m)}, M_u^{(m)}, M_w^{(m)}, M_v^{(m)}$	=	elements of the linear stability operator used in Eqs. (20) and defined in the Appendix
U	=	velocity at boundary-layer edge
$\hat{u}_1, \hat{v}_1$	=	flow modification amplitude functions
$\bar{u}_3$	=	amplitude function of the disturbance velocity field [Eq. (17)]
$\bar{v}$	=	total velocity field in the stability analysis
$\bar{v}_0 = (u_0, w_0, v_0), p_0$	=	reference flow velocity and pressure fields
$\bar{v}_1 = (u_1, 0, v_1), p_1$	=	velocity and pressure modifications caused by wall suction
$\bar{v}_2, p_2$	=	mean modified flow and pressure fields
$\bar{v}_3$	=	disturbance velocity field
$\bar{w}_3$	=	amplitude function of the disturbance velocity field [Eq. (18)]
$\bar{x}$	=	position vector (x, z, y)
Y	=	wall-normal coordinate in the transformed (computational) domain
y	=	wall-normal coordinate made dimensionless with δ^*
y_{edge}	=	edge of boundary layer
y_0	=	transformation parameter required in the numerical solution (see Secs. II and III.B)
Z_n	=	derivatives of Φ (see Sec. II)
α	=	streamwise wave number of flow disturbance and/or wall suction
β	=	pressure gradient parameter in the Falkner–Skan equation
γ	=	suction parameter in the Falkner–Skan equation
δ	=	Floquet exponent
δ^*	=	dimensional displacement thickness
η	=	similarity variable in the Falkner–Skan equation
λ_n	=	roots of characteristic equation in the solution describing flow modifications outside boundary layer
μ	=	spanwise wave number of flow disturbance
$\sigma = \sigma_r + i\sigma_i$	=	complex amplification rate
Φ	=	stream function amplitude function [Eq. (5)]
ψ	=	stream function of the mean modified flow [Eq. (5)]
$\bar{\omega}$	=	total vorticity field in the stability analysis
$\bar{\omega}_2$	=	vorticity field of the modified mean flow
$\bar{\omega}_3$	=	disturbance vorticity field

Subscript

*	=	dimensional quantities

I. Introduction

THE laminar-turbulent transition process in boundary layers results from the growth of small disturbances. This growth is described by the classical linearized operator and can have two forms. The asymptotic growth (as $t \to \infty$) is described by the eigenvalues of this operator. The flow is considered stable if there are no unstable eigenvalues. Even if all eigenvalues are stable, disturbances can be subject to an initial growth, so-called transient growth, as a result of the interdependence of various linear modes associated with the nonnormality of the operator. The transient growth might be sufficient to bring disturbances to the level where they can trigger a bypass transition. Although these issues are well understood in the case of ideal, parallel flows,[1] very little is known about them even in the case of slightly different flows.

The asymptotic instability in boundary layers has the form of traveling wave instability. The critical disturbances have the form

Received 1 May 2001; revision received 1 November 2001; accepted for publication 6 November 2001.

*Graduate Student, Department of Mechanical and Materials Engineering.
†Professor, Department of Mechanical and Materials Engineering. Associate Fellow AIAA.

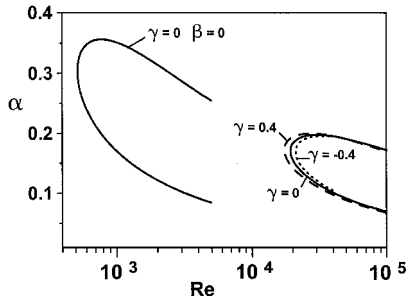

Fig. 1 Neutral stability curves describing the traveling wave (TS) instability in the Blasius as well as in the Falkner–Skan boundary layers with pressure gradient corresponding to $\beta = 5$ and with three levels of suction corresponding to $\gamma = -0.4, 0, +0.4$.

of two-dimensional waves traveling in the downstream direction and are frequently referred to as the Tollmien–Schlichting (TS) waves. In the case of the Blasius boundary layer, these waves begin to grow when the Reynolds number based on the displacement thickness reaches a value of about 520. Reed et al.[2] provide a good description of the various processes associated with this instability. It is known that boundary layers with favorable pressure gradients, such as those exemplified by the Falkner–Skan flows, are much more stable. Results shown in Fig. 1 demonstrate that the critical Reynolds number increases from $Re_{cr} \approx 520$ to about $Re_{cr} \approx 2 \times 10^4$ as the Falkner–Skan pressure-gradient parameter increases from $\beta = 0$ to 5.

As a result, these boundary layers rarely attract attention when considering laminar airfoil designs but are nevertheless very important as they describe flow conditions close to the leading edge of an airfoil. If such flows cannot be kept stable, it is not likely that the flow farther downstream can be kept laminar.

Transient growth in boundary layers has attracted a lot of attention more recently.[3,4] The available results indicate that the most significant growth is associated with streamwise vortices. This growth is reduced by applying favorable pressure gradient as compared to the boundary layer with a constant pressure.[5,6]

Boundary layers close to the leading edge are very thin, and thus very small surface corrugation (surface roughness) can significantly alter their stability properties. The area around the leading edge of an airfoil cannot be kept perfectly smooth in real operating conditions, and thus one must look for methods of flow stabilization that can balance the effect of surface corrugations. Surface suction is an accepted tool for flow stabilization and has been used for decades in the aerospace industry. The best known stabilization mechanism involves modifications of the mean velocity distribution through application of uniform suction. Such suction leads to the reduction of the growth rates of the TS waves.[7] In the case of a highly accelerated boundary layer, such as in the case of $\beta = 5$, the critical Reynolds number changes from $Re_{cr} = 1.75 \times 10^4$ in the presence of fairly strong blowing corresponding to Falkner–Skan suction parameter $\gamma = 0.4$ to $Re_{cr} = 2.11 \times 10^4$ in the presence of fairly strong suction with $\gamma = -0.4$, as illustrated by the results shown in Fig. 1. Cathalifaud and Luchini[8] demonstrated that suction can also be used to minimize transient growth of disturbances.

The wave subtraction principle[9] represents an alternative flow stabilization technique. It involves suction in the form of a properly selected traveling wave that "cancels" the undesired TS wave. This mechanism has not been investigated in the case of accelerated boundary layers. Although the introduction of suction waves can lead to the reduction/elimination of undesired disturbances, it can also lead to the creation of new instabilities.[10]

In practice, uniform suction is impossible to achieve,[11] and thus one must determine the boundaries for the acceptable level of suction nonuniformities. It might be necessary to increase the average level of suction in order to compensate for the potentially undesirable effects of such nonuniformities.

Nonuniform surface suction can be introduced intentionally as a nonintrusive method for flow control. In this case one is interested in identifying the optimal properties of suction distribution (that is, the form of the "smallest" suction that produces the "largest" changes in the flow). A very large range of flow responses can be achieved by taking advantage of the near-resonant and/or forced types of responses.[12] A properly selected suction might also force the flow system through the stability limit, if such a limit exists, opening a new range of opportunities for flow manipulation.[10]

Distributed surface suction can be viewed as an analog of distributed surface roughness. It has been shown in the case of channel flow that the flow instability caused by such suction is qualitatively similar to flow instabilities caused by surface corrugation.[10,13] Analysis of stability of accelerated boundary layers modified by nonuniform surface suction can thus offer an insight into dynamics of accelerated boundary layers over corrugated surfaces, such as those found near the leading edge of airfoils.

Floryan[14] considered the boundary layer with constant pressure and was able to show that infinitesimally small suction nonuniformities can interfere with the TS waves only if they contain suction waves with the same or nearly the same wave number and phase speed as the neutral TS waves. Roberts et al.[15] considered small but finite suction nonuniformities and were able to demonstrate that such nonuniformities can induce an instability that leads to the formation of streamwise vortices. The present paper describes extension of the latter analysis to the case of accelerated boundary layers. The focus is on the asymptotic instability (that is, as $t \to \infty$), the normal modes approach is used, and the problem is posed as an eigenvalue problem.

This paper is organized as follows. Section II describes the reference flow: two-dimensional self-similar boundary layer modified by suction nonuniformity. The boundary layer with pressure parameter $\beta = 5$ has been selected for detailed analysis to underscore the fact that an instability can occur even in boundary layers with a very strong favorable pressure gradient. Section III is devoted to the analysis of stability of the boundary layer modified by suction. Section IV gives a summary of the main conclusions.

II. Boundary Layer Modified by Nonuniform Suction/Blowing

Consider flow over a semi-infinite flat plate overlapping with the positive x axis, as shown in Fig. 2. In the absence of suction nonuniformities, the fluid motion is described by

$$\bar{v}_0(\bar{x}, t) = (u_0, w_0, v_0) = \left(\frac{\mathrm{d}F}{\mathrm{d}\eta}, 0, 0\right), \qquad P_0(\bar{x}, t) = p_0(x) \tag{1}$$

where the function F is described by the Falkner–Skan equation in the form

$$\frac{\mathrm{d}^3F}{\mathrm{d}\eta^3} + F\frac{\mathrm{d}^2F}{\mathrm{d}\eta^2} - \gamma\frac{\mathrm{d}^2F}{\mathrm{d}\eta^2} + \beta\left[1 - \left(\frac{\mathrm{d}^2F}{\mathrm{d}\eta^2}\right)^2\right] = 0$$

$$F = \frac{\mathrm{d}F}{\mathrm{d}\eta} = 0 \quad \text{at} \quad \eta = 0, \qquad \frac{\mathrm{d}F}{\mathrm{d}\eta} \to 1 \quad \text{as} \quad \eta \to \infty \tag{2}$$

In the preceding, positive β corresponds to the favorable pressure gradient and negative (positive) γ describes the wall suction (blowing). The effects of boundary-layer growth are neglected. There is experimental evidence suggesting that these effects are not important except in the case of high-frequency disturbances.[16] Figure 3 illustrates distributions of $u_0(y)$ for the Blasius boundary layer as well as for accelerated boundary layer with $\beta = 5$ for three levels of suction/blowing (for example, $\gamma = -0.4, 0, +0.4$). The distance normal to the plate y is scaled using the displacement thickness δ^*

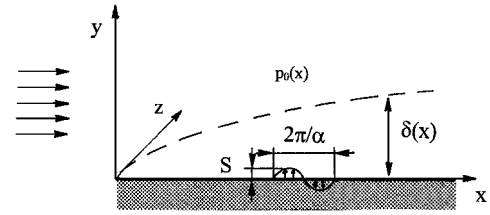

Fig. 2 Sketch of the flow domain.

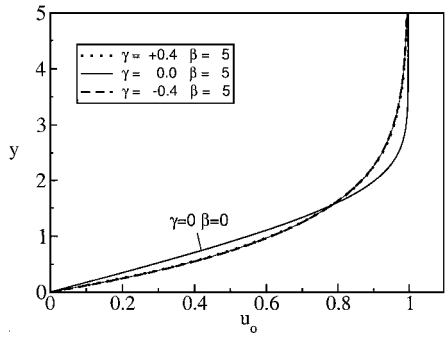

Fig. 3 Distribution of the streamwise velocity component $u_0(y)$ in the Falkner–Skan boundary layer with pressure gradient corresponding to $\beta = 5$ and with three levels of suction corresponding to $\gamma = -0.4, 0, +0.4$. Velocity distribution of Blasius boundary layer ($\beta = 0, \gamma = 0$) is given for reference purposes.

defined as

$$\delta^* = \int_0^\infty \left(1 - \frac{u_0^*}{U^*}\right) \mathrm{d}y^*$$

We shall use displacement thickness δ^* as the length scale in the rest of this paper.

At the wall we apply periodic suction in the form

$$v(x, z, 0) = S\cos(\alpha x) = \tfrac{1}{2} S e^{i\alpha x} + \mathrm{CC} \tag{3}$$

where S is real, CC stands for the complex conjugate, and i denotes the imaginary unit. Because the analysis shall be limited to small suction amplitudes, the suction distribution [Eq. (3)] can be viewed as representing a typical Fourier mode in an arbitrary suction distribution that does not result in a net mass flux.

The mean modified flowfield can be represented as

$$\bar{v}_2(\bar{x}) = \bar{v}_0(\bar{x}) + \bar{v}_1(\bar{x}) = [u_0(y), 0, 0] + [u_1(x, y), 0, v_1(x, y)]$$
$$p_2(\bar{x}) = p_0(x) + p_1(x, y) \tag{4}$$

where the wall-normal velocity component of the unmodified flow has been neglected. Substituting Eq. (4) into the two-dimensional Navier–Stokes and continuity equations, eliminating pressure, linearizing the resulting equations for small suction amplitudes S, subtracting the undisturbed flow quantities, introducing a stream function in the form $u_1 = \partial\psi/\partial y$, $v_1 = -\partial\psi/\partial x$, and assuming the solution to be in the form

$$\psi(x, y) = \Phi(y)e^{i\alpha x} + \mathrm{CC}, \qquad u_1(x, y) = \hat{u}_1(y)e^{i\alpha x} + \mathrm{CC}$$
$$v_1(x, y) = \hat{v}_1(y)e^{i\alpha x} + \mathrm{CC} \tag{5}$$

leads to the following problem to be solved numerically:

$$D^4\Phi + \left(-2\alpha^2 - i\alpha Re u_0\right)D^2\Phi + \left(\alpha^4 + i\alpha^3 Re u_0 + i\alpha D^2 u_0\right)\Phi = 0 \tag{6a}$$

$$\Phi = \frac{iS}{2\alpha}, \qquad D\Phi = 0 \qquad \text{at} \qquad y = 0 \tag{6b}$$

$$\Phi \to 0, \qquad D\Phi \to 0 \qquad \text{as} \qquad y \to \infty \tag{6c}$$

In the preceding, Re stands for Reynolds number based on the displacement thickness and $D = \mathrm{d}/\mathrm{d}y$. A linear model of flow modifications is sufficient for suction amplitudes capable of inducing flow instability.[10] Assumption (5) is consistent with the assumed form of the wall suction [for example, with Eq. (3)].

The rate at which flow modifications decay as $y \to \infty$ can be deduced by noting that u_0 becomes constant as $y \to \infty$ and coefficients in Eq. (6a) become constant. The solution outside the boundary layer takes the form

$$\Phi = \sum_{n=1}^{n=4} c_n e^{\lambda_n y} \tag{7}$$

$$\lambda_1 = \alpha, \qquad \lambda_2 = \sqrt{\alpha^2 + iRe\alpha}, \qquad \lambda_3 = -\lambda_1, \qquad \lambda_4 = -\lambda_2 \tag{8}$$

Because real parts of $\lambda_{1,2}$ are positive, the constants $c_{1,2}$ must be zero in order for flow modifications to vanish far away from the wall.

The problem has been solved using two methods. The first method takes advantage of the availability of an analytical solution (7) outside the boundary layer. Equation (6a) is rewritten as a system of first-order equations in the form

$$DZ_1 = Z_2, \qquad DZ_2 = Z_3, \qquad DZ_3 = Z_4$$
$$DZ_4 = (2\alpha^2 + i\alpha Re)Z_3 - (\alpha^4 + i\alpha^3 Re)Z_1 \tag{9}$$

where $Z_1 = \Phi$. Solution of Eq. (9) is written as

$$Z_n = \sum_{k=1}^{k=4} A_{\mathrm{nk}} c_k e^{\lambda_k y}, \qquad A_{\mathrm{nk}} = \lambda_k^{n-1} \tag{10}$$

and boundary conditions corresponding to Eq. (6c) are posed as

$$A_{\mathrm{nk}}^{-1} Z_n = 0, \qquad n = 1, 2 \qquad \text{at} \qquad y = y_{\mathrm{edge}} \tag{11}$$

where y_{edge} is sufficiently large so that approximation (9) of the original problem (6a) is valid. The actual value of y_{edge} has to be selected through numerical experimentation and depends of the form of the undisturbed boundary layer (that is, it depends on the values γ). At the wall the relevant boundary conditions have the form

$$Z_1 = iS/2\alpha, \qquad Z_2 = 0 \qquad \text{at} \qquad y = 0 \tag{12}$$

Equation (6a) has been integrated numerically between $y = y_{\mathrm{edge}}$ and $y = 0$ using a standard integrator. This approach provides a better control of numerical accuracy than the method based on mapping discussed next. Unfortunately, it cannot be easily extended to the stability analysis of the modified flow where the analytical solution outside the boundary layer is not readily available.

The second method involves mapping of the half-infinite domain $y \in [0, \infty]$ onto a strip $Y \in [0, 1]$ using the transformation $Y = \exp(-y/y_0)$. The transformed equations are discretized using a spectral Chebyshev Tau method. The method is similar to the one described by Casalis,[17] and its detailed description is omitted from this presentation. Typically, $N = 80$ Chebyshev polynomials are used in the computations. Parameter y_0 is used to control the density of the collocation points in the neighborhood of the wall. Variation of this parameter from $y_0 = 4$ to 40 results in the reduction of the number of points placed inside the displacement thickness from about 50% to about 25%. Correct selection of y_0 requires extensive testing because the character of the solution changes very rapidly as a function of flow parameters and especially as a function of the wave number α (Figs. 4 and 5). When α is small, the gradients inside the boundary layer are fairly small, and the flow modifications extend far beyond the boundary layer. As a result, a fairly small number of points inside the boundary layer is sufficient, but a larger number of points is required outside the boundary layer. For high values of α, flow modifications are concentrated inside the boundary layer and decay rapidly outside. As a result, one needs to place larger number of points inside the boundary layer. Leaving too many points outside the boundary layer leads to a near singular matrix and problems with the roundoff error. Comparisons of both methods as well as systematic studies of the effects of N and y_0 permit us to establish the correct values of the mapping parameter y_0 (see Sec. III.B for details).

III. Linear Stability of the Modified Flow

This section considers the linear stability of boundary-layer flow modified by nonuniform wall suction. Because of the assumed magnitude of the suction nonuniformities, the flow modifications induced by the suction form a part of the basic state. The basic state is no longer parallel; it has a spatial structure that has to be accounted for. The linear stability of this basic state is considered next.

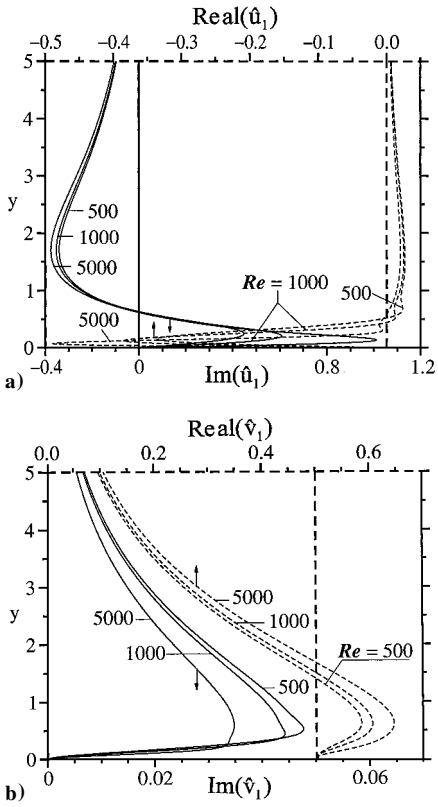

Fig. 4 Variation of the flow modifications induced by periodic suction with the wave number $\alpha = 0.5$ as a function of the Reynolds number for the Falkner–Skan boundary layer with $\beta = 5$ and $\gamma = 0$: a) $\hat{u}_1(y)$ and b) $\hat{v}_1(y)$; —— and - - -, imaginary and real parts, respectively. All results are normalized with $S = 1$.

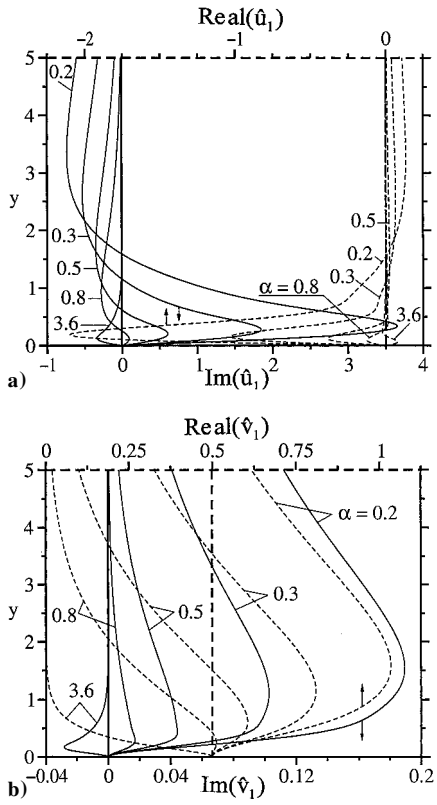

Fig. 5 Variation of the flow modifications induced by periodic suction as a function of the suction wave number α for the Falkner–Skan boundary layer with $\beta = 5$ and $\gamma = 0$ and with Reynolds number $Re = 10^3$: a) $\hat{u}_1$ (y) and b) $\hat{v}_1(y)$; —— and - - -, imaginary and real parts, respectively. All results are normalized with $S = 1$.

A. Problem Formulation

Problem formulation is analogous to the one given in Ref. 10. The following presentation is limited to a short outline. The analysis begins with the governing equations in the form of vorticity transport and continuity equations:

$$\frac{\partial \bar{\omega}}{\partial t} - (\bar{\omega}\cdot\nabla)\bar{v} + (\bar{v}\cdot\nabla)\bar{\omega} = \frac{1}{Re}\nabla^2\bar{\omega} \tag{13a}$$

$$\nabla\cdot\bar{v} = 0 \tag{13b}$$

$$\bar{\omega} = \nabla\times\bar{v} \tag{13c}$$

Unsteady, three-dimensional disturbances are superimposed on the mean part in the form

$$\bar{\omega} = \bar{\omega}_2(x, y) + \bar{\omega}_3(x, z, y, t), \qquad \bar{v} = \bar{v}_2(x, y) + \bar{v}_3(x, z, y, t) \tag{14}$$

where subscripts 2 and 3 refer to the mean flow and the disturbance field, respectively. The assumed form [Eq. (14)] of the flow is substituted into the governing equations (13), the mean part is subtracted, and the equations are linearized. The resulting linear disturbance equations have the form

$$\frac{\partial \bar{\omega}_3}{\partial t} + (\bar{v}_2\cdot\nabla)\bar{\omega}_3 - (\bar{\omega}_3\cdot\nabla)\bar{v}_2 + (\bar{v}_3\cdot\nabla)\bar{\omega}_2 - (\bar{\omega}_2\cdot\nabla)\bar{v}_3 = \frac{1}{Re}\nabla^2\bar{\omega}_3 \tag{15a}$$

$$\nabla\cdot\bar{v}_3 = 0 \tag{15b}$$

$$\bar{\omega}_3 = \nabla\times\bar{v}_3 \tag{15c}$$

The mean flow is assumed to have the form [see Eq. (5)]

$$\bar{v}_2(\bar{x}, t) = [u_0(y), 0, 0] + \left\{[\hat{u}_1(y), 0, \hat{v}_1(y)]e^{i\alpha x} + \text{CC}\right\} \tag{16}$$

The disturbance equations have coefficients that are functions of x and y only, and thus the solution can be written in the form

$$\bar{v}_3(x, z, y, t) = \bar{u}_3(x, y)\exp[i(-\sigma t + \mu z)] + \text{CC} \tag{17}$$

The exponent μ is real and accounts for the spanwise periodicity of the disturbance field. The exponent σ is assumed to be complex, and its imaginary and real parts describe the rate of growth and the frequency of the disturbances, respectively.

Because the coefficients are periodic in x with periodicity $2\pi/\alpha$, $\bar{u}_3$ is written, following the Floquet theory,[18] as

$$\bar{u}_3(x, y) = e^{i\delta x}\bar{w}_3(x, y) = e^{i\delta x}\sum_{m=-\infty}^{m=+\infty}\bar{G}_m(y)e^{im\alpha x} \tag{18}$$

where $\bar{w}_3$ is periodic in x with the same periodicity $2\pi/\alpha$. The first equation follows from the Floquet theory, whereas the second expresses the Fourier mode decomposition. Our interest is in the temporal stability theory, and thus δ is assumed to be real. The final form of the disturbance velocity vector is written as

$$\bar{v}_3(x, z, y, t) = \sum_{m=-\infty}^{m=+\infty}\left[g_u^{(m)}(y), g_w^{(m)}(y), g_v^{(m)}(y)\right] \times \exp\{i[(\delta + m\alpha)x + \mu z - \sigma t]\} + \text{CC} \tag{19}$$

Substitution of Eqs. (16) and (19) into the disturbance equations and separation of the Fourier components results, after a rather lengthy algebra, in the system of linear differential equations governing $g_u^{(m)}$, $g_w^{(m)}$, $g_v^{(m)}$ in the form

$$T^{(m)}\left[t_m g_w^{(m)} - \mu g_u^{(m)}\right] + Re\,\mu Du_0 g_v^{(m)} = iRe\left[N_u^{(m)}g_u^{(m-1)} + N_w^{(m)}g_w^{(m-1)} + N_v^{(m)}g_v^{(m-1)} + K_u^{(m)}g_u^{(m+1)} + K_w^{(m)}g_w^{(m+1)} + K_v^{(m)}g_v^{(m+1)}\right] \tag{20a}$$

$$S^{(m)}g_v^{(m)} = -Re\left[L_u^{(m)}g_u^{(m-1)} + L_w^{(m)}g_w^{(m-1)} + L_v^{(m)}g_v^{(m-1)} + M_u^{(m)}g_u^{(m+1)} + M_w^{(m)}g_w^{(m+1)} + M_v^{(m)}g_v^{(m+1)}\right] \tag{20b}$$

$$it_m g_u^{(m)} + i\mu g_w^{(m)} + Dg_v^{(m)} = 0 \tag{20c}$$

where the explicit forms of all operators are given in the Appendix. In the case of disturbances in the form of streamwise vortices,[10] the x and y components of $\bar{w}_3$ in Eq. (18) are real, z component of $\bar{w}_3$ is purely imaginary, $g_u^{(m)} = g_u^{(-m)^*}$, $g_v^{(m)} = g_v^{(-m)^*}$, $g_w^{(m)} = -g_w^{(-m)^*}$, and the size of the system decreases by a factor of two.

Effects of flow modifications as a result of nonuniform suction are contained in the terms on the right-hand side of Eqs. (20a) and (20b). In their absence all modes from the Fourier series [Eq. (19)] decouple and Eqs. (20) describe the classical (Tollmien–Schlichting), three-dimensional instability. The coupling caused by nonuniform suction involves only three consecutive terms from the Fourier series. Equations (20) can be interpreted as representing a perturbation of the classical (Orr–Sommerfeld) linear stability operator.

Equations (20) are supplemented by the homogeneous boundary conditions and form an eigenvalue problem whose nontrivial solution exists only for certain combinations of parameters δ, σ, and μ. The required dispersion relation has to be determined numerically.

B. Numerical Solution

The problem to be solved is described by an infinite set of coupled linear homogeneous ordinary differential equations (20) with homogeneous boundary conditions. An approximate solution can be found by truncating the sum in Eqs. (20) after a finite number of M terms and solving the eigenvalue problem for a two-point boundary-value problem for $2M + 1$ differential equations of type (20). The success of this approach depends on the rate of convergence of the Fourier series. Results of tests show, for the values of suction amplitude S of interest in this analysis, that the eigenvalues can be determined with three digits accuracy with $M = 2$. Most of the calculations have been carried out with $M = 3$ as a precautionary measure.

For computational purposes the half-infinite domain $y \in [0, \infty]$ is mapped onto a strip $Y \in [0, 1]$ using the same exponential transformation $Y = \exp(-y/y_0)$ that was utilized in the determination of flow modifications induced by nonuniform wall suction (Sec. II). The transformed equations are discretized by employing the spectral Chebyshev Tau method.[17] A detailed description of this procedure is omitted from this presentation. The selection of the number of the Chebyshev polynomials N as well as the transformation constant y_0 required systematic tests. It has been determined that the eigenvalues can be determined with three digits accuracy using $N \geq 80$ over the whole range of parameters studied. The appropriate values of the mapping parameter y_0 are $y_0 = 16, 15, 12, 5$ for $\alpha = 0.2, 0.3, 0.5, \geq 1.0$, respectively.

Part of the testing of the accuracy of the numerical solution and calibration of the transformation method involved evaluation of the eigenvalues describing TS waves in a boundary layer without nonuniform suction. In such a case the right-hand sides of Eqs. (20) become zero, and equations describing mode $m = 1$ can be solved separately using a modification of the algorithm that takes advantage of the availability of an analytical solution outside the bounday layer described in Sec. II.

The spectral discretization procedure results in a matrix eigenvalue problem $Ax = 0$, where $A(\sigma)$ represents the coefficient matrix. This matrix is linear in σ, that is, $A = A_0 + A_1\sigma$, where $A_0 = A(0)$, $A_1 = A(1) - A_0$. The σ spectrum is determined by solving a general eigenvalue problem in the form $B_0 x = \sigma B_1 x$. In addition, an approach based on tracing of zeros of the determinant of A using the Newton–Raphson procedure has been implemented for determination of individual eigenvalues. Two methods for tracing of eigenvalues in the parameter space have been used. In the first method one alters flow conditions and produces an approximation for the eigenvalue, which is then improved iteratively by searching for the near by zero of the determinant using the Newton–Raphson search procedure. In the second one, the inverse iterations method, one computes an approximation for the eigenvector x_a corresponding to the unknown eigenvalue σ_a using an iterative process in the form $(B_0 - \sigma_0 B_1)x^{(n+1)} = B_1 x^{(n)}$, where σ_0 and $x^{(0)}$ are the eigenvalue and the eigenvector (an eigenpair) corresponding to the unaltered flow. If σ_a is the eigenvalue closest to σ_0, $x^{(n)}$ converges to x_a. The eigenvalue σ_a is evaluated using formula $\sigma_a = x_a^* B_0 x_a / x_a^* B_1 x_a$, where the asterisk denotes complex conjugate transpose. The inverse iterations method is generally more efficient for eigenvalue tracing.

IV. Results

We shall begin our discussion by describing changes in the Falkner–Skan boundary layer induced by periodic suction nonuniformities (with zero net mass flux). These changes include flow modifications induced directly by the suction nonuniformities as well as changes in the stability properties of the flow. We shall subsequently investigate how the overall properties of the flow can be affected by adding a uniform suction and, in particular, whether the uniform suction is an effective tool for flow stabilization when suction nonuniformities are present. Finally, we shall describe behavior of the flow subject to nonuniform blowing.

A. Boundary Layer Without Uniform Suction ($\gamma = 0$)

The forms of velocity modifications induced by suction nonuniformities are illustrated in Figs. 4 and 5. Results displayed in Fig. 4 demonstrate that the modifications do not change very rapidly as a function of the Reynolds number. Results shown in Fig. 5 demonstrate a strong effect of variations of the suction wave number α. All results are normalized with $S = 1$ for presentation purposes.

The stability analysis is focused on the temporal stability theory and disturbances characterized by the same spatial periodicity as the suction nonuniformities. Accordingly, the Floquet exponent δ is set to zero, and the exponent σ is assumed to be complex. The rate of growth of disturbances is given by $\mathrm{Im}(\sigma)$.

It is known that in the case of parallel flow approximation, the two-dimensional TS waves determine the critical stability conditions. Addition of suction nonuniformities might modify the stability characteristics either through modification of the properties of the TS waves or through creation of a new instability. Floryan[10] identified one of such instabilities and provided a preliminary discussion of its characteristics. This particular instability gives rise to disturbances in the form of streamwise, spatially modulated vortices [the dominant mode corresponds to $m = 0$ in Eq. (19)] and is completely attributable to suction nonuniformities. These vortices do not propagate, that is, $\mathrm{Real}(\sigma) = 0$. We shall now discuss properties of this instability in detail.

Figure 6 displays amplifications rates of streamwise vortices induced by suction nonuniformities for $Re = 10^3$ and 2×10^3. It can be seen that the instability might occur at flow Reynolds numbers that are by an order of magnitude smaller then those required to induce the TS waves (compare Figs. 1 and 6). The values of the Reynolds numbers and suction amplitudes required to induce this instability are very similar to those required to induce the same instability in boundary layers without pressure gradient.[15] It can be seen that there is a finite band of suction wave numbers α that gives rise to the instability, and that this band is bounded from below and from above. Each wave number α gives rise to a finite band of unstable vortex wave numbers μ. This band is also bounded from above and from below. The amplification rate of the vortices and the range of the unstable wave numbers μ increases with an increase of the Reynolds number. The maximum amplification rate shifts at the

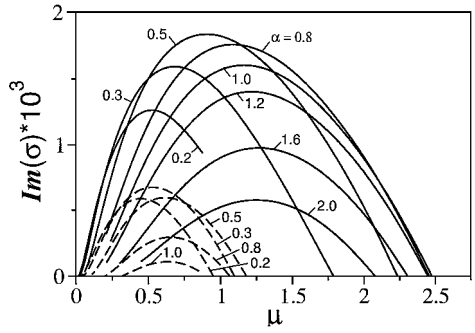

Fig. 6 Amplifications rates $\mathrm{Im}(\sigma)$ as a function of the spanwise wave number μ for disturbances in the form of streamwise vortices. The amplitude S of the suction nonuniformities is $S = 0.006$; - - - and ——, $Re = 10^3$ and 2×10^3, respectively. The results presented are for the Falkner–Skan boundary layer with $\beta = 5.0$ and $\gamma = 0$.

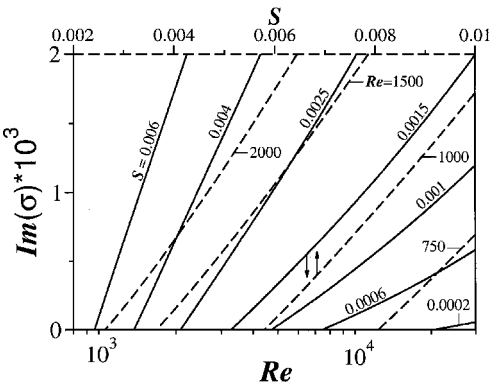

Fig. 7 Amplification rates Im(σ) as a function of the amplitude S of suction nonuniformities for the constant flow Reynolds number Re (- - -) and as a function of the flow Reynolds number Re for the constant amplitude of the suction nonuniformities (——). The results displayed are for the streamwise vortices with $\mu = 1.0$ and $\alpha = 0.8$ and for the Falkner–Skan boundary layer with $\beta = 5$ and $\gamma = 0$.

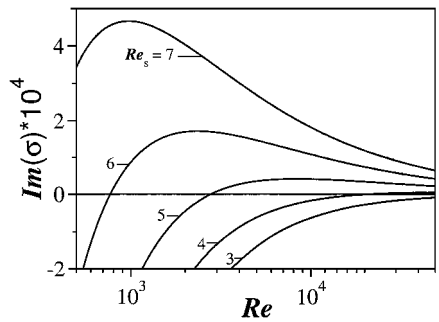

Fig. 8 Amplification rates Im(σ) as a function of the flow Reynolds number Re for different levels of suction Reynolds number Re_s. The results displayed are for the streamwise vortices with $\mu = 1.0$ and $\alpha = 0.8$ and for the Falkner–Skan boundary layer with $\beta = 5$ and $\gamma = 0$.

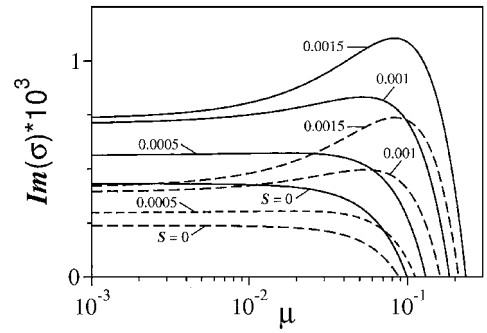

Fig. 9 Amplification rates Im(σ) for the oblique TS waves as a function of the spanwise wave number μ for different values of the amplitude of suction nonuniformities S; - - - and ——, $Re = 2.5 \times 10^4$ and 4×10^4, respectively. The results are displayed for $\alpha = 0.17$, which corresponds approximately to the critical TS wave number in the absence of suction nonuniformities. The results are for the Falkner–Skan boundary layer with $\beta = 5$ and $\gamma = 0$.

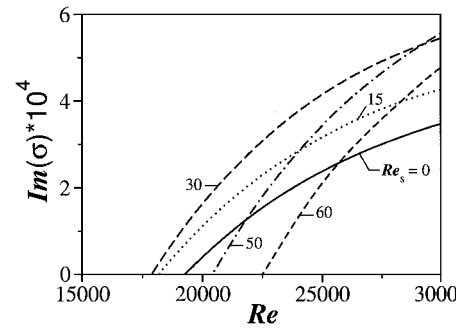

Fig. 10 Amplification rates Im(σ) of the two-dimensional TS wave with $\alpha = 0.17$ as a function of the flow Reynolds number Re for different values of the suction Reynolds number Re_s. The results presented are for the Falkner–Skan boundary layer with $\beta = 5$ and $\gamma = 0$.

same time toward the higher suction wave numbers α. The increase of the amplification with Reynolds number and suction amplitude is vividly illustrated in Fig. 7, which displays variations of Im(σ) as functions of both Re and S.

The strength of suction nonuniformities can also be measured using a suction Reynolds number defined as $Re_s = S \times Re$ rather than suction amplitude S. Figure 8 displays variations of the amplification rate as a function of Reynolds number for fixed values of Re_s. It can be seen that a general criterion which guarantees flow stability can be formulated using Re_s. In the range of parameters studied, the suction will not induce streamwise vortices as long as $Re_s \lesssim 3.7$.

We shall now discuss properties of TS waves in the presence of suction nonuniformities. The analysis is limited to those TS waves having the same periodicity in the streamwise direction as the suction nonuniformity. Figure 9 displays amplification rates of oblique TS waves computed for various suction amplitudes S. It can be seen that in the range of suction amplitudes S studied the two-dimensional TS waves remain most unstable only if S is sufficiently small. An increase of the amplitude of the nonuniformities above $S \approx 0.0005$ leads to the appearance of a band of oblique waves that have higher amplification rates then the two-dimensional waves. As illustrated in Fig. 10, an initial increase of suction nonuniformity amplitude, as measured by the suction Reynolds number Re_s, leads to a destabilization of the two-dimensional TS waves, whereas a further increase leads to their stabilization. The maximum reduction of the critical Reynolds number for such waves is of the order of 10% of its value corresponding to the case of no suction nonuniformities.

B. Boundary Layer with Nonzero Average Suction/Blowing ($\gamma = -0.4, +0.4$)

The results discussed in Sec. IV.A show that suction nonuniformities can induce a new instability in the form of streamwise vortices, whereas they have a rather insignificant effect on the TS waves. Because this instability can occur at values of Reynolds number that are by an order of magnitude smaller then those required to induce the TS waves, it is of interest to determine 1) whether the new instability can be eliminated through an increase of the average level of the suction and 2) how big the average suction should be in order to stabilize the flow completely. One can address the question of the effect of surface blowing as a part of the same analysis. Both issues shall be addressed by studying the stability of the Falkner–Skan boundary layer with suction/blowing corresponding to $\gamma = -0.4$, $+0.4$. Such values of the suction parameter represent a fairly strong suction/blowing and thus permit identification of any effects of the average suction/blowing if such an effect exists. Although the suction/blowing corresponding to $\gamma = \text{const}$ does not correspond to a constant suction, the rate of suction variations in the streamwise direction is similar to the rate of boundary-layer growth and thus can be neglected in the analysis.

The results displayed in Fig. 3 demonstrate that variations in the form of the mean velocity profile $u_0(y)$ as a function of the suction parameter γ are fairly small. Results displayed in Fig. 11 demonstrate that changes of the flow modifications induced by the suction nonuniformities as a function of the suction parameter γ are also fairly small.

Figure 12 displays amplification rates for the streamwise vortices induced by suction nonuniformities for three levels of suction/blowing (that is, for $\gamma = -0.4$, 0, $+0.4$). It can be seen that the addition of net suction/blowing has a rather small effect on the stability characteristics: the range of unstable suction wave numbers, the range of the wave numbers of the resulting vortices, the amplification rates of the vortices as well as the wave number of the most amplified vortex change very little in response to a rather significant change in the level of uniform suction. Figure 13 illustrates the effects of variations of the flow Reynolds number and the amplitude of suction nonuniformities on the amplifications rates

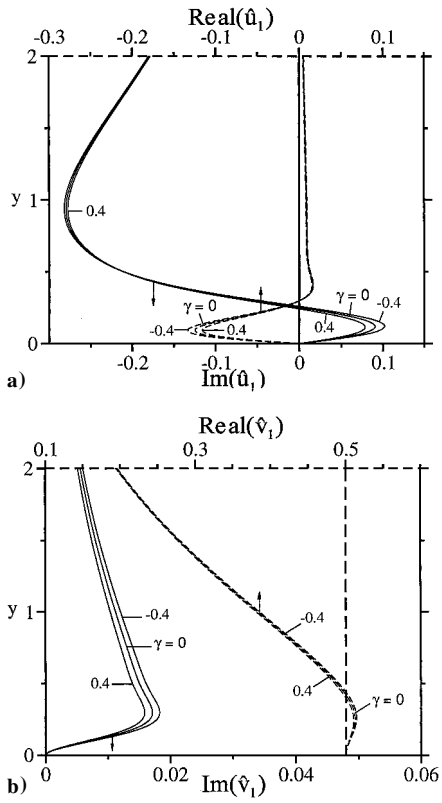

Fig. 11 Variation of the flow modifications induced by periodic suction with the wave number $\alpha = 0.8$ for the Reynolds number $Re = 10^3$ as a function of the suction parameter γ: a) $\hat{u}_1(y)$ and b) $\hat{v}_1(y)$. The results presented are for the Falkner–Skan boundary layer with $\beta = 5$; —— and - - -, imaginary and real parts, respectively. All results are normalized with $S = 1$.

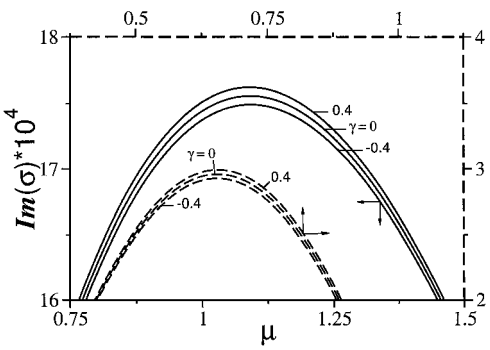

Fig. 12 Amplifications rates Im(σ) as a function of the spanwise wave number μ for disturbances in the form of streamwise vortices induced by the suction nonuniformities with the wave number $\alpha = 0.8$ and with the amplitude $S = 0.006$ for three levels of uniform suction (that is, for $\gamma = -0.4$, 0, +0.4); - - - and ——, $Re = 10^3$ and 2×10^3, respectively. The results presented are for the Falkner–Skan boundary layer with $\beta = 5$.

of the vortices for the same three levels of suction/blowing. It can be seen that in the range of parameters studied rather significant changes in the average suction/blowing have a very small effect on the amplification rates of the vortices. In all cases studied, the amplification rates increase almost linearly as a function of S and Re. The results displayed in Fig. 14 demonstrate further that the flow can be kept stable as long as $Re_s \lesssim 3.7$ regardless of the magnitude of the average suction/blowing. It can be concluded that suction is not particularly helpful in elimination of the vortices, similar to the case of crossflow problems.

The results displayed in Fig. 15 demonstrate again that the response of TS waves to the presence of suction nonuniformities is not significantly altered by changes in the average level of suction/blowing. The amplification rates decrease by at most a factor of two when strong blowing ($\gamma = 0.4$) is replaced by strong suction

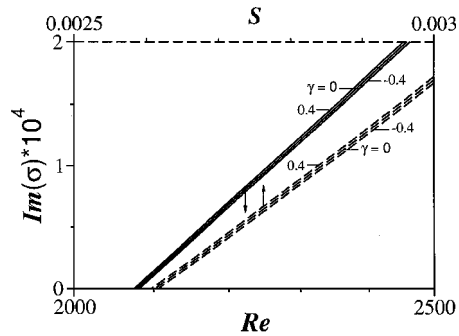

Fig. 13 Amplification rates Im(σ) as a function of the amplitude S of the suction nonuniformities for the flow Reynolds number $Re = 2 \times 10^3$ (- - -) and as a function of the flow Reynolds number Re for the suction amplitude $S = 0.0025$ (——) for three levels of uniform suction (that is, for $\gamma = -0.4$, 0, +0.4). The results displayed are for the streamwise vortices with $\mu = 1.0$ and $\alpha = 0.8$ and for the Falkner–Skan boundary layer with $\beta = 5$.

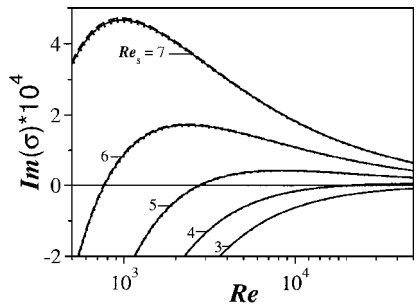

Fig. 14 Amplification rates Im(σ) as a function of the flow Reynolds number Re for different levels of suction Reynolds number Re_s. The results displayed are for the streamwise vortices with $\mu = 1.0$ and $\alpha = 0.8$ for three levels of uniform suction [that is, for $\gamma = -0.4$ (· · · ·), 0.0 (——) and +0.4 (- - -)]. The results presented are for the Falkner–Skan boundary layer with $\beta = 5$.

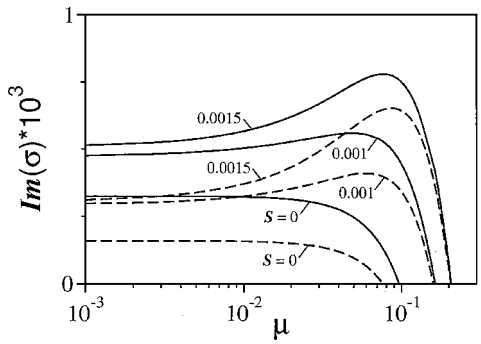

Fig. 15 Amplification rates Im(σ) for the oblique TS waves as a function of the spanwise wave number μ for different values of the amplitude S of the suction nonuniformities for $Re = 2.5 \times 10^4$ for the Falkner–Skan boundary layer with $\beta = 5$; - - - and ——, $\gamma = -0.4$ and +0.4, respectively. The results displayed are for $\alpha = 0.169$ in the former case and for $\alpha = 0.172$ in the latter case, where each wave number corresponds approximately to the critical TS wave in the absence of suction nonuniformities.

($\gamma = -0.4$). There exists a band of oblique waves with amplification rates higher than the two-dimensional waves if the suction amplitude is high enough. This dominance of the oblique waves over two-dimensional waves increases with an increasing level of suction. The results displayed in Fig. 16 demonstrate that the maximum reduction of the critical Reynolds number that can be induced by suction non-uniformities in the range of parameters studied is of the order of 10% of its value corresponding to the case of no suction nonuniformities.

The present analysis can be extended to three-dimensional boundary layers, such as those found on swept wings. It is difficult to predict whether the dominant response of such flow will have a form

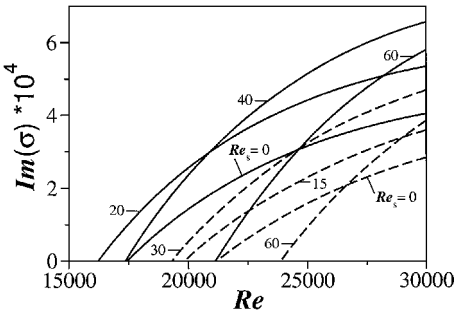

Fig. 16 Amplification rates Im(σ) of the two-dimensional TS wave as a function of the flow Reynolds number *Re* for different values of the suction Reynolds number Re_s for the Falkner–Skan boundary layer with $\beta = 5$; - - - and ——, $\gamma = -0.4$ and +0.4, respectively. The results displayed are for $\alpha = 0.169$ in the former case and for $\alpha = 0.172$ in the latter case, where each wave number corresponds approximately to the critical TS wave in the absence of suction nonuniformities.

similar to vortices found in the present study, or, perhaps, it will assume the form similar to the crossflow vortices. This question deserves further investigation.

V. Summary

Stability of accelerated boundary layers modified by a nonuniform surface suction has been considered. The boundary layers have been represented as the Falkner–Skan flows with pressure parameter $\beta = 5$. The arbitrary suction distribution has been represented in terms of Fourier series. Detailed calculations have been carried out in the case of suction distributions described by a single Fourier mode corresponding to a cosine function in the streamwise direction, with the amplitude and wave number of this function being the only parameters.

The available results show that two types of instability are possible. The first one involves the classical, traveling (Tollmien–Schlichting) waves whose amplifications rates are slightly modified by the presence of suction nonuniformities. It is shown that oblique waves become dominant for sufficiently high suction amplitudes. This result has significant consequencies for prediction of the transition location as such waves are routinely neglected on the basis of Squire's theorem.

The second instability is new and involves streamwise vortices that arise only because of the presence of the nonuniformities. This instability occurs at Reynolds numbers that are of an order of magnitude smaller that those required to induce the TS waves. This result is important for the design of laminar airfoils because the accelerated boundary layers are typically considered as being very stable. Present results show that the vortex instability occurs in the accelerated boundary layers under similar conditions as in the constant-pressure boundary layers. It is this instability that is expected to dominate the evolution of such boundary layers in the presence of suction nonuniformities.

The vortex instability can be induced by a finite band of suction wave numbers. Each particular suction wave number gives rise to a finite band of vortex (spanwise) wave numbers. The strength of the instability increases almost linearly with the amplitude of the suction nonuniformities and the flow Reynolds number. The instability does not occur in the range of parameters studied if the suction Reynolds number is $Re_s < 3.7$.

Application of a uniform suction has a negligible effect on the vortices. The available results show that if the suction-induced vortices do appear they cannot be eliminated by simply increasing the average level of suction. This has consequences for the design of transition control system utilizing surface suction. If the suction nonuniformities associated with such systems are higher then the critical threshold leading to the appearance of the vortices, the flow cannot be stabilized by a simple increase of the average suction.

Nonuniformities in surface blowing can induce an instability similar to the one induced by the surface suction. The characteristics of this instability are very similar to the characteristics of the suction-induced instability.

Appendix: Operator Definitions

Operators used in Eqs. (20) are

$$D = \frac{\mathrm{d}}{\mathrm{d}y}, \qquad t_m = \delta + m\alpha, \qquad k_m^2 = t_m^2 + \mu^2$$

$$T^{(m)} = D^2 - k_m^2 - iRe(t_m u_0 - \sigma)$$

$$S^{(m)} = \left(D^2 - k_m^2\right)^2 - iRe(t_m u_0 - \sigma)\left(D^2 - k_m^2\right) + iRe\, t_m D^2 u_0$$

$$N_u^{(m)} = -\mu t_m \hat{u}_1 + i\mu \hat{v}_1 D, \qquad N_w^{(m)} = \left(t_m^2 - \alpha t_m\right)\hat{u}_1 - i t_m \hat{v}_1 D$$

$$N_v^{(m)} = i\mu D\hat{u}_1, \qquad K_u^{(m)} = \mu\left(-t_m \hat{u}_1^* + i\hat{v}_1^* D\right)$$

$$K_w^{(m)} = \left(t_m^2 + \alpha t_m\right)\hat{u}_1^* - i t_m \hat{v}_1^* D, \qquad K_v^{(m)} = i\mu D\hat{u}_1^*$$

$$L_u^{(m)} = -t_m^2 D\hat{u}_1 + i\alpha k_m^2 \hat{v}_1 + t_m(-t_m\hat{u}_1 + iD\hat{v}_1)D + i t_m \hat{v}_1 D^2$$

$$L_w^{(m)} = \mu\left[-t_m D\hat{u}_1 + \alpha D\hat{u}_1 + (-t_m\hat{u}_1 + \alpha\hat{u}_1 + iD\hat{v}_1)D + i\hat{v}_1 D^2\right]$$

$$L_v^{(m)} = i t_m D^2\hat{u}_1 + k_m^2 D\hat{v}_1 + i t_{m-1} k_m^2 \hat{u}_1 + \left(i t_m D\hat{u}_1 + k_m^2\hat{v}_1\right)D$$

$$M_u^{(m)} = -t_m^2 D\hat{u}_1^* - i\alpha k_m^2 \hat{v}_1^* + t_m\left(-t_m\hat{u}_1^* + iD\hat{u}_1^*\right)D + i t_m \hat{v}_1^* D^2$$

$$M_w^{(m)} = \mu\left[-t_m D\hat{u}_1^* - \alpha D\hat{u}_1^* + \left(-t_m\hat{u}_1^* - \alpha\hat{u}_1^* + iD\hat{v}_1^*\right)D + i\hat{v}_1^* D^2\right]$$

$$M_v^{(m)} = i t_m D^2\hat{u}_1^* + k_m^2 D\hat{v}_1^* + i t_{m+1} k_m^2 \hat{u}_1^* + \left(i t_m D\hat{u}_1^* + k_m^2\hat{v}_1^*\right)D$$

In the preceding equations asterisks denote complex conjugate.

Acknowledgments

This work has been carried out with the support of the Natural Sciences and Engineering Research Council of Canada, Canadair, and de Haviland, Inc.

References

[1]Schmid, P. J., and Henningson, D. S., *Stability and Transition in Shear Flows*, Vol. 142, Applied Mathematical Sciences, Springer-Verlag, New York, 2001.

[2]Reed, H., Saric, W. S., and Arnal, D., "Linear Stability Theory Applied to Boundary Layers," *Annual Review of Fluid Mechanics*, Vol. 28, 1996, pp. 389–428.

[3]Andersson, P., Brandt, L., Bottaro, A., and Hennigson, D. S., "On the Breakdown of Boundary Layer Streaks," *Journal of Fluid Mechanics*, Vol. 428, Feb. 2001, pp. 29–60.

[4]Andersson, P., Berggren, M., and Henningson, D. S., "Optimal Disturbances and Bypass Transition in Boundary Layers," *Physics of Fluids*, Vol. 11, No. 1, 1999, pp. 134–150.

[5]Corbett, P., and Bottaro, A., "Optimal Perturbations for Boundary Layers Subject to Streamwise Pressure Gradient," *Physics of Fluids*, Vol. 12, No. 1, 2000, pp. 120–130.

[6]Tumin, A., "A Model for Spatial Algebraic Growth in a Boundary Layer Subjected to a Streamwise Pressure Gradient," *Physics of Fluids*, Vol. 13, No. 5, 2001, pp. 1521–1523.

[7]Schlichting, H., *Boundary Layer Theory,* 7th ed., McGraw–Hill, New York, 1979, pp. 506–510.

[8]Cathalifaud, P., and Luchini, P., "Algebraic Growth in Boundary Layers: Optimal Control by Blowing and Suction at the Wall," *European Journal of Mechanics—B/Fluids*, Vol. 19, No. 4, 2000, pp. 469–478.

[9]Biringen, S., "Active Control of Transition Using Suction-Blowing," *Physics of Fluids*, Vol. 27, No. 6, 1984, pp. 1345–1347.

[10]Floryan, J. M., "Stability of Wall-Bounded Shear Layers in the Presence of Simulated Distributed Surface Roughness," *Journal of Fluid Mechanics*, Vol. 335, March 1997, pp. 29–55.

[11]MacManus, D. G., and Eaton, J. A., "Flow Physics of Discrete Boundary Layer Suction—Measurements and Predictions," *Journal of Fluid Mechanics*, Vol. 417, Aug. 2000, pp. 45–75.

[12]Szumbarski, J., and Floryan, J. M., "Forcing of Channel Flow Using Distributed Suction—a Linear Theory," Expert Systems in Fluid Dynamics Research Lab., Rept. ESFD-1/99, Dept. of Mechanical and Materials Engineering, Univ. of Western Ontario, London, ON, Canada, 1999.

[13]Cabal, T., Szumbarski, J., and Floryan, J. M., "Stability of Flow in a Corrugated Channel," *Proceedings of the 5th IUTAM Symposium on Laminar-Turbulent Transition*, edited by H. F. Fasel and W. S. Saric, Springer-Verlag, Berlin, 2000, pp. 345–350.

[14]Floryan, J. M., "Instability of Boundary Layers in the Presence of Weak Distributed Surface Suction," Expert Systems in Fluid Dynamics Research Lab., Rept. ESFD-10/2000, Dept. of Mechanical and Materials Engineering, Univ. of Western Ontario, London, ON, Canada, 2000.

[15]Roberts, P. J. D., Floryan, J. M., Casalis, G., and Arnal, D., "Boundary Layer Instability Induced by Wall Suction," *Physics of Fluids*, Vol. 13, No. 9, 2001, pp.2543–2553.

[16]Klingman, B. G. B., Boiko, A. V., Westin, K. J. A., Kozlov, V. V., and Alfredsson, P. H., "Experiments on Stability of Tollmien-Schlichting Waves," *European Journal of Mechanics—B/Fluids*, Vol. 12, No. 4, 1993, pp. 493–514.

[17]Casalis, G., "Instabilite Secondaire de la Couche Limite Laminaire Tridimensionelle en Ecoulement Incompressible: Description du Code de Calcul.," Dept. d'Aerothermodynamique, Rapport Technique 63/5618.54, CERT/ONERA, Toulouse, France, 1991.

[18]Coddington, E. A., and Levinson, N., *Theory of Ordinary Differential Equations*, McGraw–Hill, New York, 1965.

P. J. Morris
Associate Editor